Thermal Behavior of a Novel Solar Hybrid Road for Energy Harvesting

Domenico Vizzari, Jean Dumoulin, Emmanuel Chailleux, Eric Gennesseaux, Stéphane Lavaud, Stéphane Bouron, Jean-Luc Manceau

Journal of Testing and Evaluation

doi:10.1520/JTE20220283 available online at www.astm.org

Domenico Vizzari,[1] Jean Dumoulin,[2] Emmanuel Chailleux,[2] Eric Gennesseaux,[2] Stéphane Lavaud,[2] Stéphane Bouron,[2] and Jean-Luc Manceau[2]

Thermal Behavior of a Novel Solar Hybrid Road for the Energy Harvesting

Reference

D. Vizzari, J. Dumoulin, E. Chailleux, E. Gennesseaux, S. Lavaud, S. Bouron, and J.-L. Manceau, "Thermal Behavior of a Novel Solar Hybrid Road for the Energy Harvesting," *Journal of Testing and Evaluation* https://doi.org/10.1520/JTE20220283

ABSTRACT

Transportation is undergoing a radical transformation toward a novel way of thinking about road pavement: a sustainable, multifunctional infrastructure able to satisfy mobility needs, ensuring high safety standards, low carbon impact, automated detection through smart sensors, and resilience against natural and anthropogenic hazards.

In this scenario, the road could also play a role for energy harvesting, thanks to the exploitation of solar radiation. The latter can be directly converted into electricity by solar cells placed under a semitransparent layer, or it can be harvested through a calorific flowing fluid. The aim of this paper is to introduce the concept of "hybrid road," which is able to exploit both approaches. The innovative pavement is a multilayered structure composed by a semitransparent top layer made of glass aggregates bonded together thanks to a semitransparent resin, an electrical layer containing the solar cells, a porous asphalt layer for the circulation of the calorific fluid, and finally, a base waterproof layer.

The hybrid road can generate electricity, contrast the heat-island effect, exploit the harvested energy to run a heat pump for heating purposes, or facilitate road deicing during winter.

The present paper details experimental data obtained through energetic tests performed with a laboratory-size prototype of the hybrid road. The results show that the prototype is able to harvest around 55.2 W through the heat-transfer fluid. Furthermore, the heat exchange between water and asphalt has a cooling effect on the entire prototype.

Keywords

thermal behavior, energy harvesting, electric output, solar road, hybrid road, porous asphalt

Manuscript received June 1, 2022; accepted for publication August 25, 2022; published online xxxx xx, xxxx.

[1] University Gustave Eiffe, All. des Ponts et Chaussées, Bouguenais (Nantes) 44340, France (Corresponding author), e-mail: domenico.vizzari@univ-eiffel.fr, https://orcid.org/0000-0002-9878-053X

[2] University Gustave Eiffel, All. des Ponts et Chaussées, Bouguenais (Nantes) 44340, France

Introduction

The road of the next generation is a sustainable, multifunctional infrastructure able to satisfy mobility needs, ensuring high safety standards, low carbon impact, automated detection through smart sensors, and resilience against natural and anthropogenic hazards. Furthermore, the road could contribute to the energy needs and play the role of novel energy harvesting technology.

Energy harvesting[1] is the process by which energy is captured and stored, exploiting an external source (e.g., solar power, thermal energy, wind energy, electromagnetic ambient energy, kinetic energy, etc.).

The road infrastructure has good potential as an energy harvesting system because it is exposed daily to solar radiation, and it does not require the use of additional land. The solar radiation can be directly converted into electric power thanks to the photovoltaic effect. This solution, named photovoltaic road, consists of solar cells placed under a semitransparent layer. This latter has to support the traffic load, guarantee the vehicle friction, and allow the passage of the sunlight to the lower layer.[2] Full-scale applications of solar roads can be found in Tourouvre au Perche (France)[3] and in Jinan (China),[4] where 1 km of road can generate 1,000 MWh and 280 MWh per year, respectively.

Another example of energy harvesting is the asphalt solar collectors; they consist of pipes embedded into the asphalt, able to extract heat energy through a fluid (i.e., water). Because of the temperature gradient between the fluid and the asphalt, a heat-transfer process occurs from pavement to fluid. The asphalt solar collectors allow for the reduction of the temperature of the pavement, mitigating the heat asphalt and slowing down the rutting. The extracted energy is usually used as a snow-melting system[5] or in heating for buildings.[6] Recently, some researchers investigated the possibility of replacing the asphalt solar collectors with a porous medium. Pascual-Muñoz et al.[7] proposed a multilayered pavement in which the heat-exchanger fluid passed through a porous asphalt mixture. They observed that the lower the hydraulic conductivity is, the lower the collected energy is. Asfour et al.[8] developed a two-dimensional thermo-hydraulic model to simulate the heat exchanges between the fluid and the pavement. The conclusion was that the temperature at the surface strictly depends on the hydraulic conductivity, the injection temperature of the fluid, and its calorific capacity.

Le Touz et al.[9] developed a multi-physics finite element method model of a multilayered asphalt pavement. The model combined thermal diffusion, hydraulic convection, and radiative transfer. The authors evaluated the harvested energy of the porous medium for different locations in France. The efficiency of the porous layer ranged between 31.1 % and 41 %, and it can increase by 7 % by using a semitransparent surface instead of the typical coarse aggregate.

Xiang et al.[10] combined solar road and soil heat storage technology. During the day, the sunlight is converted into electricity by the solar cells. The electricity is used to drive a pump, and the remaining part is stocked in an accumulator. At the same time, the pipes placed below the solar road absorb the heat through a heat-transfer fluid. The soil absorbs the heat and it cools the fluid, which is pumped back into the pipes. Furthermore, the authors developed a mathematical model to investigate the influence of flow rate, soil thermal properties, collector area, and borehole depth on electrical and thermal behavior of the system.

As a complement, we can also mention the thermoelectric effect as an alternative to solar cells to produce electricity.[11,12]

In academia, Hasebe, Kamikawa, and Meiarashi[13] coupled a thermoelectric generator (TEG) with an asphalt solar collector. The idea is to put in contact the hot side of the TEG with the warm water of the asphalt solar collector and the cold side with the water coming from a low-temperature source (i.e., river). Alternatively, the heat of the asphalt pavement can be conducted to the hot side of the TEG through an aluminum plate embedded into the road. In this case, the difference of temperature is given by the aluminum and a cold source such a heat sink. The latter is filled with water, and it is installed in the subsoil.[14]

The novelty of this paper is the merging of a photovoltaic road with a porous asphalt layer to maximize the exploited/collected energy. The porous asphalt has a double task: stocking the excess of heat through the water and alleviating the increase in temperature of the solar cell and of the asphalt. The advantages are for the

mechanical performance of the asphalt, which sharply declines at high temperature (loss of stiffness modulus and rutting resistance) and for the efficiency of the solar cell.

In the following paragraphs, we introduce the concept of "hybrid road." We list the materials used for the construction of a prototype, and we present the results obtained with an experimental setup for the evaluation of energy harvesting and the electrical output in lab conditions.

The Concept of Hybrid Road

The hybrid road is a multilayered pavement able to harvest energy from solar radiation. From the top to the bottom (fig. 1), the pavement is composed by the following four components: a semitransparent top layer made of glass aggregates bonded together through a semitransparent resin; an electrical layer containing the solar cells; a porous asphalt layer sandwiched between two waterproofing bituminous membranes, typically used to prevent concrete bridge deterioration; and a high-modulus asphalt mixture, characterized by longer durability, superior rutting resistance, and satisfactory fatigue resistance.

The hybrid road is able to generate electricity thanks to the solar cells and harvest heat energy at the same time through the water circulated in the porous layer. Furthermore, the semitransparent layer favors a kind of "greenhouse effect," in which the solar radiation penetrates into the porous medium, maximizing the harvested energy.

The Test Method

The prototype of the hybrid road evaluated in the present paper has dimensions of 70 cm × 20 cm × 14 cm (fig. 2).

The semitransparent surface has a 1-cm thickness made up by glass aggregates bonded together through an epoxy glue. The volume fractions are 57 % of 4/6 mm glass aggregates, 38 % of 2/4 mm, and 5 % of glue.

The glue is a two-component epoxy called Araldite 2020, which is usually used for glass bonding. The glue properties are as follows: viscosity, 150 mPa.s; pot life, 45 min; fixture time, 960 min; shear strength, 16 MPa; elongation at break, 4 %; Young modulus, 2,800 MPa; and working temperature range, −40–60°C.

For the glue preparation, the two components are weighted according to the ratio of 100:35, and they are manually mixed together for two min and poured into the glass aggregates. The preparation continues by mixing the glue and glass aggregates for some minutes until they are homogeneous.

The manufacture procedure of the semitransparent layer consists of the following steps: (1) Weigh each class of aggregates according to the volume fractions; (2) mix the glass aggregates and the glue for 3 min using a lab spoon; (3) lay down the mixture, respecting the thickness of 1 cm; (4) apply a low manual compaction to obtain a uniform surface; and (5) store the semitransparent layer for at least 24 h at the temperature of 20°C.

FIG. 1 Three-dimensional (3D) sketch of the hybrid road.

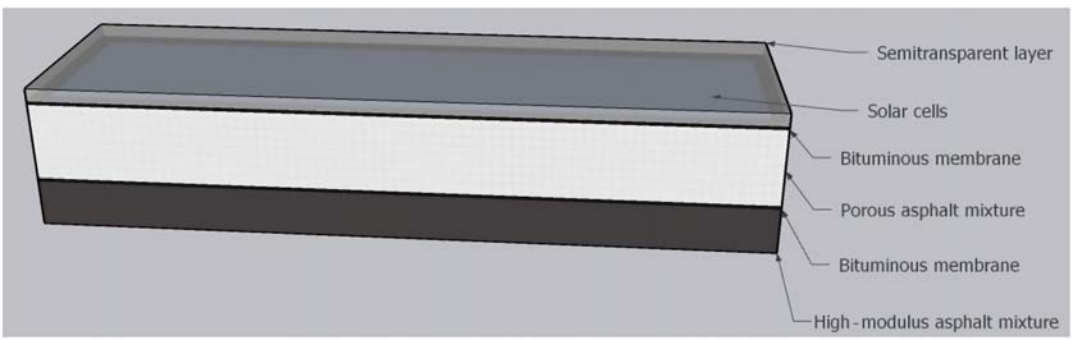

FIG. 2 Dimensions of the prototype.

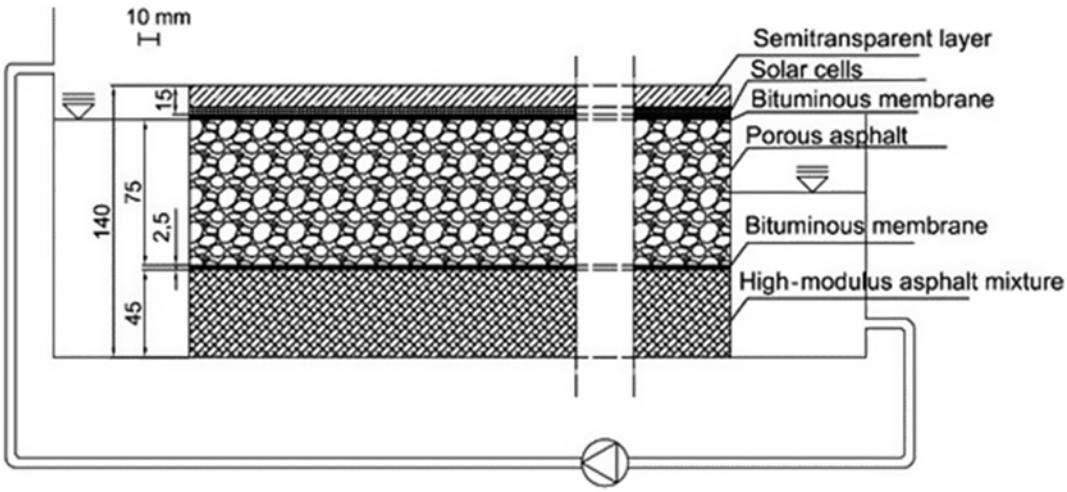

Under static load, the semitransparent layer can withstand 6.25 MPa with no damage for the solar cell.[15]

The solar cell is monocrystalline silicon with dimensions of 11 cm × 11 cm × 0.3 cm. Based on the lab measurement performed at 1,000 W/m^2, the peak power is 1.1 W, the open circuit voltage is 3.68 V, and the short circuit current is 0.43 A.

The power loss of the solar cell is 52.9 % and 76.6 % for 1-cm and 2-cm thicknesses of semitransparent layer, respectively. The measurements refer to the early stage when there are not aging phenomena.

The porous asphalt has a thickness of 7.5 cm, bituminous content of 4.5 %, and porosity of 22.5 %. The latter is calculated based on the vacuum sealing method (ASTM D7063/D7063M-11, *Standard Test Method for Effective Porosity and Effective Air Voids of Compact Bituminous Paving Mixture Samples* [Superseded]).[16] The specimen is submerged underwater and weighed in both sealed and unsealed conditions.

To guarantee the waterproofing of the porous asphalt, the medium is sandwiched between two bituminous membranes having a thickness of 0.25 cm.

The base is a high-modulus asphalt mixture having 4.5 cm of thickness. The grading curves of both mixtures are detailed in **figure 3**.

The Experimental Setup

The objective of the experiment is to study the thermal behavior of the prototype, evaluate the harvested energy, and calculate the electric power generated from the solar cell. At this scope, a dedicated test bench (**fig. 4*B*–4*D***) has been constructed. The equipment is composed of the following: (1) a halogen lamp of 1,500 W able to simulate the solar radiation; (2) a waterproof test bench to place the prototype; (3) two water collectors, corresponding to the inlet and the outlet of the prototype; (4) an insulated tank to collect the water; (5) a system of tubes that connects the water collectors to the tank; (6) a heat exchanger for the regulation of the water temperature in the tank; (7) a pump for the reinjection of the water from the tank to the inlet of the prototype; (8) a pyranometer to measure the solar radiation generated from the lamp; (9) a dedicated instrumentation to measure the intensity-voltage curve of the solar cell; (10) eight temperature sensors (**fig. 4*A***) (three placed in the interface semitransparent layer/solar cell, three in the interface bituminous membrane/porous asphalt, and two sensors placed in the inlet and the outlet of the prototype); and (11) a multichannel data logger to record the temperature of the sensors during experiments.

FIG. 3 Grading curves of the porous and high-modulus asphalt.

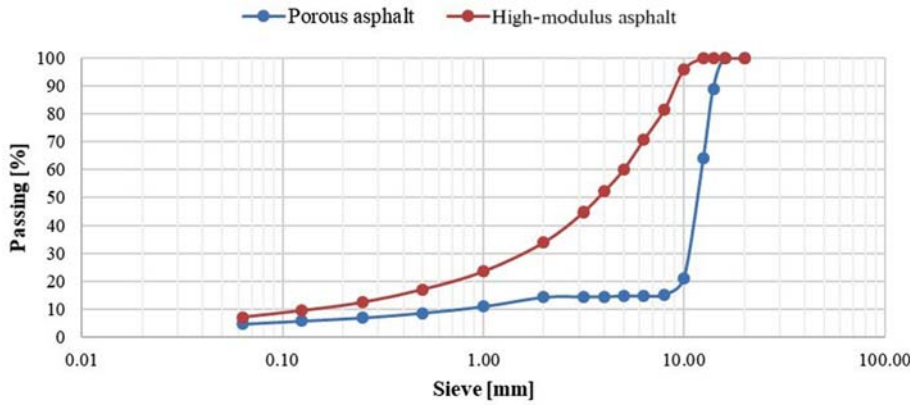

Thermal Behavior and Harvested Energy

The hybrid road is able to harvest energy thanks to the gradient of temperature between the heat-transfer fluid and the porous medium. In terms of heat exchange mechanisms, the energy is firstly balanced along the interface between surface and atmosphere. In this case, the heat flux is caused by the incident radiation of the sunlight, the convection between prototype surface and air, and the thermal radiation of the surface. In return, the heat flux causes a change of temperature in the prototype (thermal diffusion), leading at the end to a convection mechanism in the interface porous medium-fluid.

The harvested energy from the heat-transfer fluid is given by formula (1):

$$E = \rho_f C_{p,f} Q \cdot T \tag{1}$$

where:

ρ_f = the density of the fluid, kg/m^3 (≈ 1,000 Kg/m^3 for the water),

$C_{p,f}$ = the specific heat capacity of the fluid, J/Kg · K (≈ 4,180 J/Kg · K for the water),

Q = the volumetric water flow through the porous medium, m^3/s, and

ΔT = the difference of temperature between the inlet and the outlet of the prototype, K.

To measure Q and ΔT, the prototype is placed in the waterproof test bench with a slope of 1 %, and it is exposed to the radiation of a lamp. The test bench is equipped with two collectors, corresponding to the inlet and the outlet of the prototype. The water (having a temperature of 20°C) passes from the first tank to the porous asphalt, in which the convection mechanism takes place. The result is an increase of the water temperature along the path until the outlet of the second collector. At the outlet, the water has a temperature of 20 + ΔT, and it goes in the tank. The latter is equipped with a heat exchanger and is able to maintain the temperature of the water at 20°C. At this point, the pump reinjects the water from the aquarium to the inlet of the porous medium, and the cycle starts again.

The cycle is in equilibrium when the hydraulic load ΔH is constant during time (fig. 4*A*). In more detail, the water flow is regulated so that the height of the water $H1$ in the first collector corresponds to the height of the porous asphalt.

In this condition, the water flow is 0.0172 l/s.

The test is based on two different approaches: (1) simulating a quasi-permanent regime with a constant radiation illumination of 1,000 W/m^2 during 6 h and (2) simulating a periodic regime of day-night cycles with the lamp through a sinusoidal law.

FIG. 4 Hybrid road drawings: (*A*) disposition of the thermocouples; (*B*) schema of the bench test; (*C*) picture of the bench test; and (*D*) 3D sketch of the bench test.

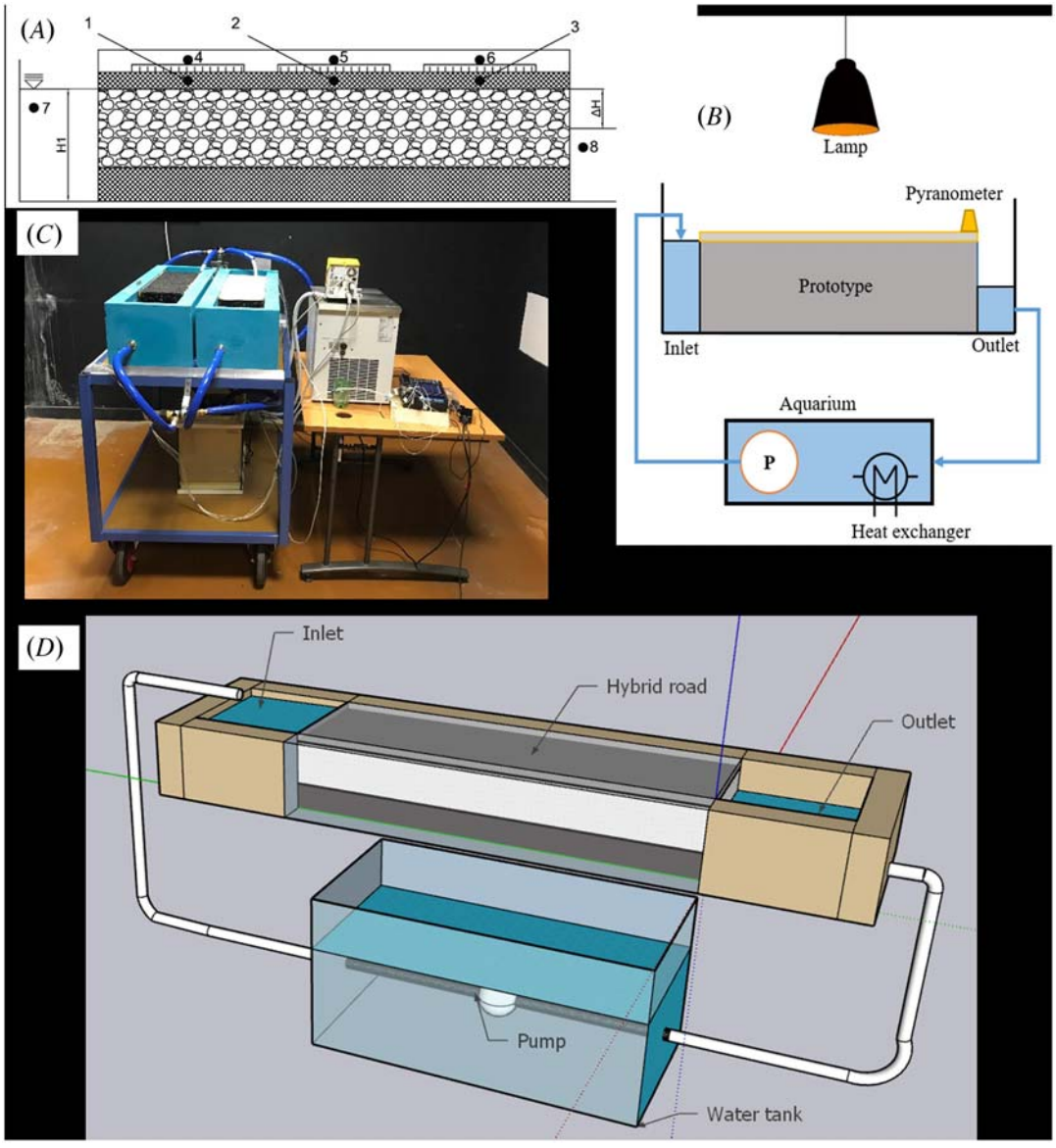

The power of the lamp is adjusted according to the pyranometer measurement. For example, when the lamp is at the maximum power, the pyranometer detects 16 mV, which corresponds to 1,733 W/m^2 (1 W/m^2 ≈ 9.27 μV). Taking in consideration the setup configuration, in which the pyranometer is placed on the corner of the prototype, the equivalent radiation in the center of the prototype is given, in first rough approximation, by the inverse square law[17]:

$$I_2 = I_1 \frac{d_1^2}{d_2^2} \tag{2}$$

where:

I_1 = the radiation intercepted by the pyranometer, W/m^2,

I_2 = the radiation in the center of the surface prototype, W/m^2,

d_1 = the distance lamp-pyranometer, m, and

d_2 = the distance lamp-center of the surface prototype, m.

Assuming $I1 = 1{,}733$ W/m^2, $d_1 = 1.02$ m, and $d_2 = 1.09$ m, the radiation in the center of the surface prototype is around 1,518 W/m^2.

Following the same approach, 1,000 W/m^2 corresponds to 45 % of the maximum power delivered from the lamp. More details about the pyranometer calibration are in the work of Le Touz, Toullier, and Dumoulin,[18] where the authors derived the distribution of solar radiation on the surface of a solar road by performing a bicubic interpolation on nine measurement points.

PSEUDO PERMANENT REGIME: CONSTANT RADIATION

The following section analyzes the results of the test at constant radiation (1,000 W/m^2 for 6 h). Figure 5 refers to the case with water flow, and it shows the variation of temperature detected from the thermocouples.

The differences of temperatures between the thermocouples are because of their different positions in the prototype. For example, thermocouple 5 detects the highest temperature (around 55°C) because it is placed in the interface semitransparent layer/solar cell along the vertical between the lamp and the surface. Thermocouple 1 detects the lowest temperature (around 38°C after 6 h) because it is placed close to the inlet of the prototype. In that zone, the porous medium is better water-saturated than the side of the outlet. Consequently, there is a better heat exchange between water and asphalt.

It is worth noting how thermocouple 8 registers higher values of temperature than the 7. It means that the convection mechanism takes place, leading to a difference of temperature between the inlet and the outlet of the prototype.

At 3 h and 36 min, all the thermocouples detect a little peak of temperature, probably because of the interference of the sunlight coming from the window located near the bench test. At 4 h and 12 min, the prototype reaches the temperature equilibrium, and all the curves settle on constant values.

Figure 6 refers to the test without water flow. As expected, the thermocouples register higher temperatures in comparison to the test with water flow. In other terms, the heat exchange between water and asphalt has a cooling effect on the entire prototype. After 6 h, the prototype does not reach the equilibrium, and the trends of the curves suggest that the temperature could increase.

Table 1 shows the change of temperature because of the absence of water. The temperature can increase by up to 51.6 %.

Figure 7 shows the harvested energy of the prototype. Because the water flow is always constant, the curve follows the trend of the ΔT curve.

FIG. 5 Temperature variation of the thermocouples with water flow through the porous asphalt.

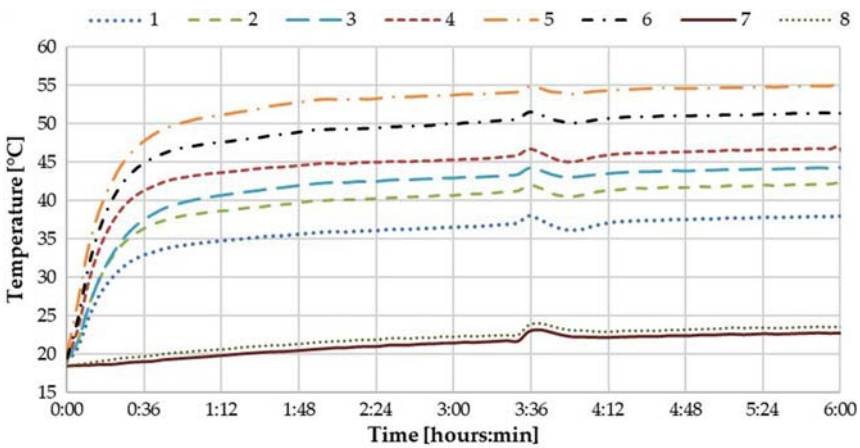

FIG. 6 Temperature variation of the thermocouples without water flow.

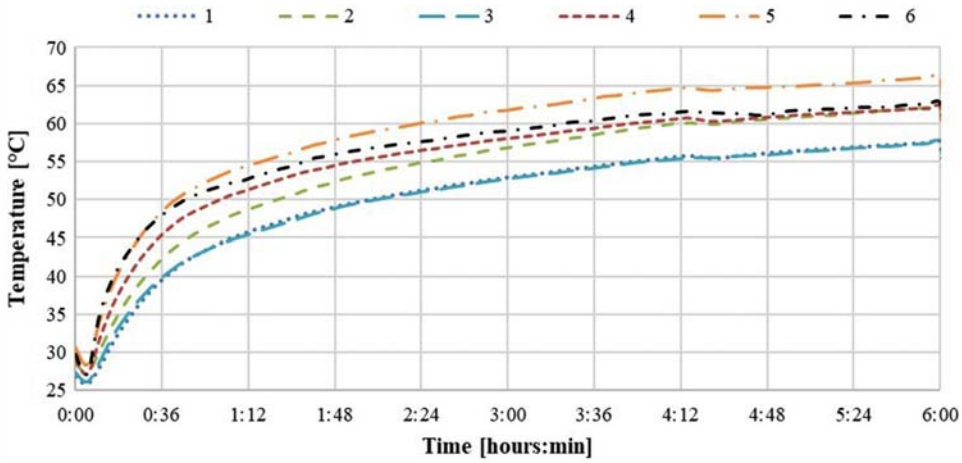

TABLE 1
Thermocouples temperatures after 6 hours test

AQ20

AQ21

	1	2	3	4	5	6
T, °C (with water flow)	38.0	42.1	44.3	46.8	54.9	51.4
T, °C (without water flow)	57.6	62.2	57.5	62.1	66.2	62.7
% increase	51.6	47.7	29.9	32.8	20.5	21.9

FIG. 7 Harvested energy of the prototype through the water.

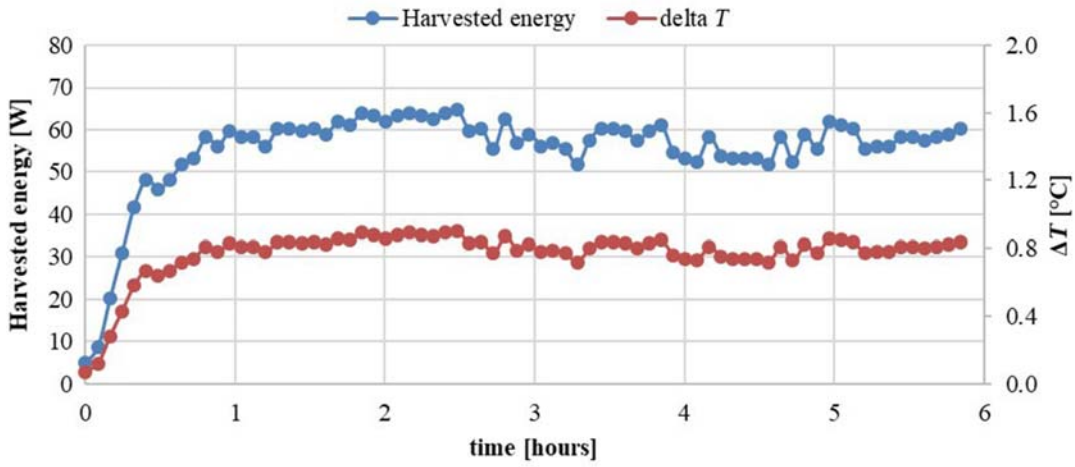

The average value of harvested energy power at 6 h is 55.2 W. The solar radiation intercepted from the surface of the prototype is around 120 W; consequently, the efficiency is around 46 %. This result is consistent with the literature. For instance, the multilayered asphalt pavement as an active solar collector of Pascual-Muñoz et al.[7] has an efficiency between 35 % and 45 % (in the case of a porous layer with 23 % of air voids and solar irradiation between 300 W/m^2 and 440 W/m^2). The comparison could be extended to the asphalt solar collectors.

FIG. 8 Temperature variation of the thermocouples for the day-night cycles.

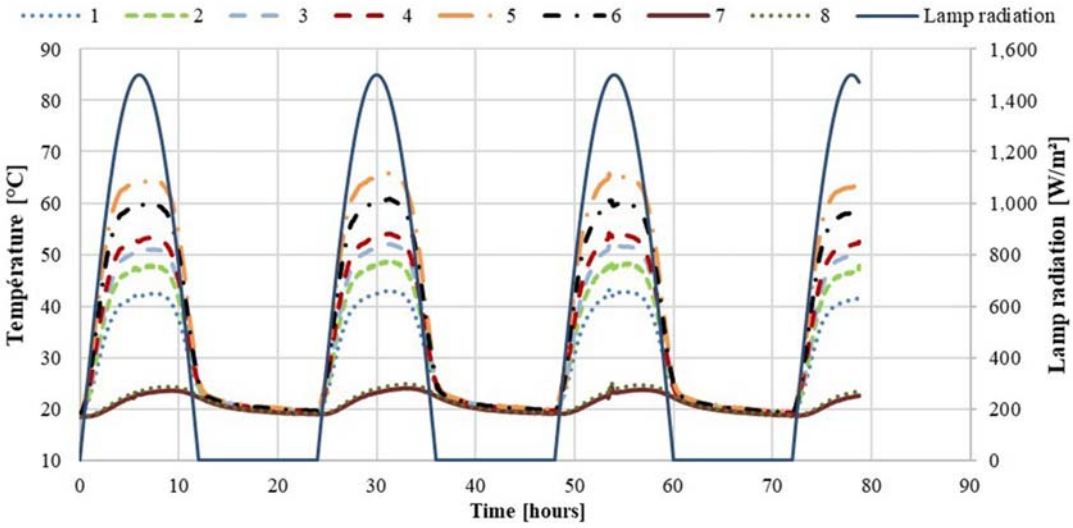

In this case, the efficiency depends on the geometry of the collector, the thickness of the asphalt above the collector, the heat-transfer properties of the materials, the inlet fluid temperature, and the water flow.[19] According to Shaopeng, Mingyu, and Jizhe,[20] the efficiency is around 33 %, while Masoumi, Tajalli-Ardekani, and Golneshan[21] obtained up to 45 % based on neural network modeling.

PERIODIC REGIME: DAY-NIGHT CYCLES

The objective of the day-night cycles is to simulate in lab condition the variation of the solar radiation. Each cycle is 24 h (12 h light + 12 h night), and the peak of the signal is at 90 % of the maximum power delivered from the lamp, which corresponds to a radiation of around 1,500 W/m^2 (fig. 8).

As for the test at constant radiation, the temperature of the thermocouple is strictly dependent on its position in the prototype. The highest temperature is detected by thermocouple 5 (around 65°C), and the peak of each curve corresponds to the peak of the lamp signal.

To avoid plastic deformation in the prototype, the test has been performed only with water flow.

FIG. 9 Harvested energy and ΔT of the prototype for the day-night cycles.

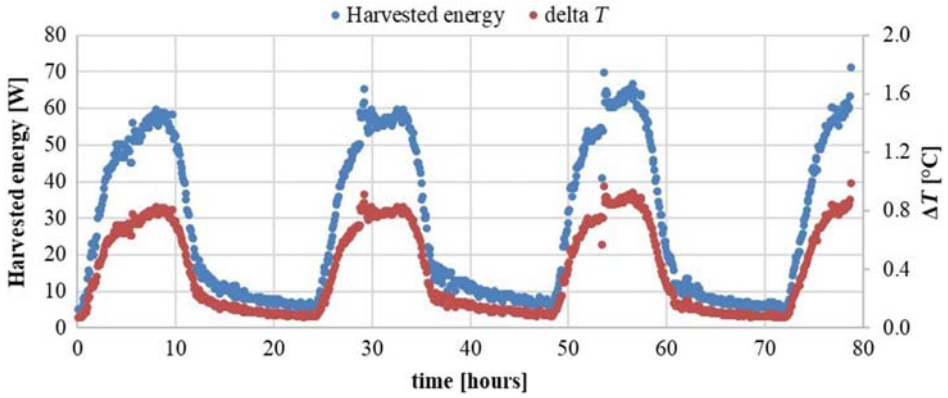

In terms of harvested energy, the average thermal power is 26.4 W per cycle of 24 h (fig. 9). For a comparison with the test at constant radiation, it is possible to analyze the harvested energy falling in an interval time of 6 h, centered at the pick of the sinusoidal signal of the lamp. In this case, the thermal power is 54.5 W per cycle, very close to the value of 55.2 W, which was obtained at a constant radiation of 1,000 W/m^2. This means that the test at constant radiation is reliable for the evaluation of the harvested energy. Moreover, it is less time-consuming.

Electric Output of the Solar Cell

As it is well known, there is an inverse correlation between the efficiency of a solar cell and its temperature. If the water flow can relieve the temperature of the prototype, can the solar cell benefit from this effect? To answer the question, the electric output of the solar cell has been monitored for 6 h at 1,000 W/m^2 with and without water flow.

The electric output of the solar cell is given by its maximum power point (*MPP*). The *MPP* is obtained from the intensity-voltage curve. It represents the maximum of the product between intensity and voltage, and it is the bias potential at which the solar cell outputs the maximum power.[22] The intensity-voltage curve is measured by an in-house measurement system, which is able to simultaneously detect the intensity and the voltage by automatically changing the electrical resistances. Every 5 minutes, a dedicated software builds the curves and generates a file with the raw data. Figure 10 shows all the intensity-voltage curves traced during 6 h in absence of water flow. Over time, the curve tends to shrink because of the reduction of efficiency of the solar cell because of the increasing temperature.

At first, the MPP is calculated for the solar cell (MPP_{solar_cell}), and the same measurement is repeated once the solar cell is merged in the semitransparent layer ($MPP_{prototype}$). The latter interacts with the solar radiations intercepted from the solar cell, causing a sharp reduction in the *MPP*.

The power loss of the solar cell is given by the following expression:

$$PL = \frac{(\varepsilon_{\text{solar\_cell}} - \varepsilon_{\text{prototype}})}{\varepsilon_{\text{solar\_cell}}} \quad (3)$$

where:

$$\varepsilon = \frac{\text{MPP}}{A \cdot I} 100\,\% \quad (4)$$

ε_{solar_cell} = the efficiency of the solar cell, %,

$\varepsilon_{prototype}$ = the efficiency of the solar cell covered by the prototype, %,

FIG. 10 Intensity-voltage curves of the solar cell during 6 h at 1,000 W/m^2 without water flow.

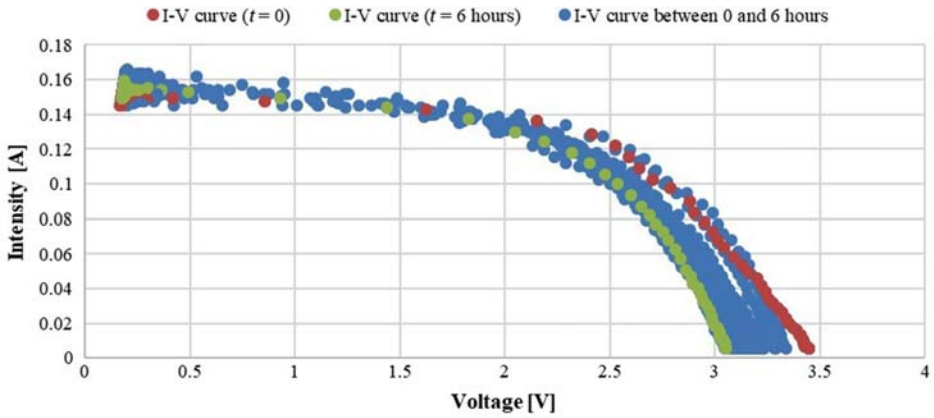

A = the surface of the solar cell, m^2 ($\approx$ 0.0121 m^2), and

I = the flux density of the solar radiation generated by the lamp, W/m^2 ($\approx$ 1,000 W/m^2).

The *PL* is calculated at $t = 0$ h and $t = 6$ h, for which the solar cell is at the minimum and maximum temperatures, respectively.

Taking into account the average measurements of thermocouples 2 and 5 and the *MPP* at $t = 0$ h and t = 6 h, the reference values are listed in Table 2.

The difference of temperature at $t = 0$ h between the test with and without water flow is because of the presence of water at 20°C in the porous medium and the absence of cooling system in the laboratory.

It is worth noting that the *MPP* values refer only to the solar cell surface. Hypothetically, the whole prototype surface (0.14 m^2) could be covered with solar cells. In the case of water flow, the *MPP* would be 2.18 W, which if added to the average thermal power of 55.2 W (see the section titled "PSEUDO PERMANENT REGIME: CONSTANT RADIATION") would give a total power of 57.38 W.

In terms of efficiency and power loss, the results are summarized in Table 3.

The reduction of efficiency at $t = 0$ h is related to the difference of temperature, similarly at $t = 6$ h. Considering the variation of power loss between $t = 0$ h and $t = 6$ h, the water flow has a slight relief effect on the temperature of the prototype, which translates into a ΔPL of 2.2 %.

The measurements of power loss are consistent with the state-of-art. Hu et al.[23] proposed a semitransparent layer made of glass aggregates and unsaturated polyester resin, having a power loss between 76 % and 83 %. A novel way to improve the transparency of the semitransparent layer is to use the surface dressing treatment.[24] It consists of a thin film of transparent glue covered with a single layer of glass aggregates. Thanks to the low thickness and high glue content, the resulting power loss is around 13–15 %.

An agreement is observed for the calculated experimental performances with the ones obtained by using the formula of Evans,[25] in which the variation of efficiency is related to the temperature of the solar cell:

$$\varepsilon_c = \varepsilon_{T_{\text{ref}}}[1 - \beta_{\text{ref}}(T_c - T_{\text{ref}})] \tag{5}$$

$$\beta_{\text{ref}} = \frac{1}{T_0 - T_{\text{ref}}} \tag{6}$$

In more detail:

ε_c = the efficiency of the solar cell, % (i.e., $\varepsilon_{prototype}(t = 6\text{ h})$),

ε_{Tref} = the efficiency at the temperature of reference, % (i.e., $\varepsilon_{prototype}$ $(t = 0\text{ h})$),

β_{ref} = the temperature coefficient of the solar cell, 1/°C,

T_c = the temperature of the solar cell, °C (i.e., T_{max} of Table 2),

TABLE 2
Reference values of temperature and MPP

Water Flow		No Water Flow	
$t = 0$ h	$t = 6$ h	$t = 0$	$t = 6$ h
$T_{min} = 19.7$°C	$T_{max} = 54.9$°C	$T_{min} = 29.6$°C	$T_{max} = 64.2$°C
$MPP_{(t=0\text{ h})} = 0.317$ W	$MPP_{(t=6\text{ h})} = 0.293$ W	$MPP_{(t=0\text{ h})} = 0.31$ W	$MPP_{(t=6\text{ h})} = 0.274$ W

TABLE 3
Efficiency and power loss of the solar cell

	$\varepsilon_{solar-cell}$	$\varepsilon_{prototype}$ $(t = 0\text{ h})$	PL $(t = 0\text{ h})$	$\varepsilon_{prototype}$ $(t = 6\text{ h})$	PL $(t = 6\text{ h})$	$\Delta PL = \text{PL}(t = 0\text{ h}) - \text{PL}(t = 6\text{ h})$
Water flow	9.15	2.62	71.4 %	2.42	73.6 %	2.2 %
No water flow	9.15	2.56	72 %	2.27	75.2 %	3.2 %

TABLE 4
Efficiency and power loss based on the formula of Evans

	$\varepsilon_{(t=0\ \mathrm{h})}$	$T_{ref(t=0\ \mathrm{h})}$, °C	$Tc_{(t=6\ \mathrm{h})}$, °C	B, 1/°C	$\varepsilon_{(t=6\ \mathrm{h})}$	$PL_{(=6\ \mathrm{h})}$
Water flow	2.62 %	19.7	49.6	0.003995	2.30 %	74.8 %
No water flow	2.56 %	29.6	64.2	0.00416	2.19 %	76.1 %

T_{ref} = the reference temperature for the solar cell, °C, (i.e., T_{min} of Table 2), and

T_0 = the temperature at which the efficiency of the solar cell drops to 0, °C (for monocrystalline ≈ 270°C).

The model slightly overestimates the power loss of the solar cell after 6 h (Table 4). The reason could be the position of the thermocouples, which are not directly in contact with the solar cells and could overestimate the values Tc and T_{ref}. Furthermore, the value of T_0 has not been measured but simply derived from the literature. Moving from these assumptions, the model could fit the experimental power loss if Tc and T_{ref} refer to thermocouple 5 and if T_0 is around 340°C.

Conclusions

The hybrid road is a multilayered pavement able to harvest energy from solar radiation.

The innovation is merging a photovoltaic road with a porous asphalt to maximize the exploited/collected energy. The idea is to add novel functionalities to the road and moderate the negative effects of extreme events thanks to the temperature control through the water in the porous layer.

The objective of this paper is to understand the variations of the temperature in the prototype, calculate the harvested energy thanks to the water pumped through the porous asphalt, and evaluate the power loss of the solar cell.

The results show that the heat exchange between water and asphalt has a cooling effect on the entire prototype. In more detail:

- The cooling effect is bigger for the thermocouples placed close to the inlet. In that zone, the water saturation is better than the zone beside the outlet. By the same logic, the thermocouples placed lower into the prototype matrix record lower temperatures.
- In absence of water flow, the temperature can increase by up to 51.6 %, increasing the risk of rutting in the asphalt.
- In terms of energy harvesting, the hybrid road has an efficiency of 46 %. The efficiency can be improved in two ways: increasing the difference of temperature between the inlet and the outlet (ΔT) or improving the water flow.
- The ΔT can be enhanced by improving the thermal effusivity of the porous medium. The thermal effusivity represents the ability of a material to exchange thermal energy with its surroundings. The water flow can be increased by improving the permeability of the porous medium, which is strictly dependent on the porosity and the tortuosity.
- Regarding the electric output, there is a direct correlation between the increase of power loss of the solar cell and the increase of temperature. In absence of water flow, the PL is around 72 % at $t = 0$ h. As the temperature of the prototype increases, after 6 h the power loss reaches 75.2 %. If the same test is performed with water flow, the power loss drops to 73.6 %. In other terms, the solar cell works better thanks to the cooling effect of the water. Despite this relief effect, the PL stands at high values because of the poor transparency of the semitransparent layer.
- The low electric power could be useful to make turn the water in the porous medium, and the moderate efficiency of the system could be compensated by the surface extension all along the road network.

Moving from these considerations, further research will focus on the optimization of the prototype. In the second generation of hybrid road, the thickness of the semitransparent layer could be reduced by using the surface

dressing technique, the epoxy replaced by transparent polyurethane, and the porous asphalt by porous concrete with higher porosity.

References

1. F. Duarte and A. Ferreira, "Energy Harvesting on Road Pavements: State of the Art," *Proceedings of the Institution of Civil Engineers – Energy* 169, no. 2 (May 2016): 79–90, https://doi.org/10.1680/jener.15.00005.
2. H. Hu, D. Vizzari, X. Zha, and R. Roberts, "Solar Pavements: A critical Review," *Renewable and Sustainable Energy Reviews* 152 (December 2021): 111712, https://doi.org/10.1016/j.rser.2021.111712
3. Colas, "Technical Datasheet," Colas, 2019, https://web.archive.org/web/20220907152109/https://www.wattwaybycolas.com/media/documents/documents-en-anglais/2019_gb_technical-datasheet-ww.pdf
4. S. Hanley, "China Opens 1-Kilometer Long Solar Road," CleanTechnica, 2017, http://web.archive.org/web/20220907152349/https://cleantechnica.com/2017/12/30/china-opens-1-kilometer-long-solar-road/
5. D. Vizzari, E. Gennesseaux, S. Lavaud, S. Bouron, and E. Chailleux, "Pavement Energy Harvesting Technologies: A Critical Review," *RILEM Technical Letters* 6 (August 2021): 93–104, https://doi.org/10.21809/rilemtechlett.2021.131
6. V. Bobes-Jesus, P. Pascual-Muñoz, D. Castro-Fresno, and J. Rordiguez-Hernandez, "Asphalt Solar Collectors: A Literature Review," *Applied Energy* 102 (February 2013): 962–970, https://doi.org/10.1016/j.apenergy.2012.08.050
7. P. Pascual-Muñoz, D. Castro-Fresno, P. Serrano-Bravo, and A. Alonso-Estébanez, "Thermal and Hydraulic Analysis of Multilayered Asphalt Pavements as Active Solar Collectors," *Applied Energy* 111 (November 2013): 324–332, https://doi.org/10.1016/j.apenergy.2013.05.013
8. S. Asfour, F. Bernardin, E. Toussaint, and J.-M. Piau, "Hydrothermal Modeling of Porous Pavement for Its Surface De-freezing," *Applied Thermal Engineering* 107 (August 2016): 493–500, https://doi.org/10.1016/j.applthermaleng.2016.06.138
9. N. Le Touz, J. Dumoulin, and J.-M. Piau, "Multi-physics FEM Model of Solar Hybrid Roads for Energy Harvesting Performance Evaluation in Presence of Semi-transparent or Opaque Pavement Surface Layer," in *International Heat Transfer Conference 16* (Ankara, Turkey: International Centre for Heat and Mass Transfer, 2018), 1809–1816, https://doi.org/10.1615/IHTC16.cms.023896
10. B. Xiang, X. Cao, Y. Yuan, M. Hasanuzzaman, C. Zeng, Y. Ji, and L. Sun, "A Novel Hybrid Energy System Combined with Solar-Road and Soil-Regenerator: Sensitivity Analysis and Optimization," *Renewable Energy* 129 (December 2018): 419–430, https://doi.org/10.1016/j.renene.2018.06.027
11. X. Zhu, Y. Yu, and F. Li, "A Review on Thermoelectric Energy Harvesting from Asphalt Pavement: Configuration, Performance and Future," *Construction and Building Materials* 228 (December 2019): 116818, https://doi.org/10.1016/j.conbuildmat.2019.116818
12. K. S. Ong, L. Jiang, and K. C. Lai, "Thermoelectric Energy Conversion," in *Comprehensive Energy Systems* (Amsterdam, The Netherlands: Elsevier, 2018), 794–815., https://doi.org/10.1016/B978-0-12-809597-3.00433-8.
13. M. Hasebe, Y. Kamikawa, and S. Meiarashi, "Thermoelectric Generators Using Solar Thermal Energy in Heated Road Pavement," in *2006 25th International Conference on Thermoelectrics* (New York: Institute of Electrical and Electronics Engineers (IEEE), 2006), 697–700, https://doi.org/10.1109/ICT.2006.331237
14. U. Datta, S. Dessouky, and A. T. Papagiannakis, "Harvesting thermoelectric energy from asphalt pavements," *Transportation Research Record: Journal of the Transportation Research Board* (2017): 12–22, https://doi.org/10.3141/2628-02
15. S. Bouron, E. Chailleux, A. Themeli, J. Dumoulin, and C. Ropert, "Revêtement translucide pour la production d'énergie électrique," *Revue générale des routes et de l'aménagement (RGRA)* 949 (2017): 76–79.
16. *Standard Test Method for Effective Porosity and Effective Air Voids of Compacted Bituminous Paving Mixture Samples (Superseded)*, ASTM D7063/D7063M-11 (West Conshohocken, PA: ASTM International, approved June 1, 2011), https://doi.org/10.1520/D7063_D7063M-11
17. J. R. S. Brownson, "Laws of Light," in *Solar Energy Conversion Systems* (Oxford, UK: Academic Press, 2014), 41–66, https://doi.org/10.1016/B978-0-12-397021-3.00003-X.
18. N. Le Touz, T. Toullier, and J. Dumoulin, "Infrared Thermography Applied to the Study of Heated and Solar Pavement: From Numerical Modeling to Small Scale Laboratory Experiments," in *Proceedings of Thermosense: Thermal Infrared Applications XXIX* (Bellingham, WA: The International Society for Optics and Photonics, 2017), 1021413, https://doi.org/10.1117/12.2262778
19. Q. Gao, Y. Huang, M. Li, Y. Liu, and Y. Y. Yan, "Experimental Study of Slab Solar Collection On the Hydronic System of Road," *Solar Energy* 84, no. 12 (December 2010): 2096–2102, https://doi.org/10.1016/j.solener.2010.09.008
20. W. Shaopeng, C. Mingyu, and Z. Jizhe, "Laboratory Investigation into Thermal Response of Asphalt Pavements as Solar Collector by Application of Small-Scale Slabs," *Applied Thermal Engineering* 31, no. 10 (July 2011): 1582–1287, https://doi.org/10.1016/j.applthermaleng.2011.01.028
21. A. P. Masoumi, E. Tajalli-Ardekani, and A. A. Golneshan, "Investigation on Performance of an Asphalt Solar Collector: CFD Analysis, Experimental Validation and Neural Network Modeling," *Solar Energy* 207 (September 2020): 703–719, https://doi.org/10.1016/j.solener.2020.06.045

22. D. Rekioua and E. Matagne. *Optimization of Photovoltaic Power Systems: Modelization, Simulation and Control* (London: Springer, 2012), https://doi.org/10.1007/978-1-4471-2403-0
23. H. Hu, X. Zha, Z. Li, and R. Lv, "Preparation and Performance Study of Solar Pavement Panel Based on Transparent Resin-Concrete," *Sustainable Energy Technologies and Assessments* 52, Part B (August 2022): 102169, https://doi.org/10.1016/j.seta.2022.102169
24. D. Vizzari, E. Gennesseaux, S. Lavaud, S. Bouron, and E. Chailleux, "Surface Dressing Treatment for Applications on Solar Roads," in *ISBM 2020: Proceedings of the RILEM International Symposium on Bituminous Materials* (Cham, Switzerland: Springer, 2021), 1719–1725, https://doi.org/10.1007/978-3-030-46455-4_218
25. S. Dubey, J. N. Sarvaiya, and B. Seshadri, "Temperature Dependent Photovoltaic (PV) Efficiency and Its Effect on PV Production in the World – a Review," *Energy Procedia* 33 (2013): 311–321, https://doi.org/10.1016/j.egypro.2013.05.072